JOURNAL OF MATERIALS SCIENCE 27 (1992) 6440–6446

Valency of copper in 123 oxides

N. S. RAMAN, B. VISWANATHAN, T. K. VARADARAJAN
Department of Chemistry, Indian Institute of Technology, Madras 600 036, India

The valency of copper in freshly prepared as well as *in situ* high-temperature oxygen-treated 123 oxides was analysed by X-ray photoelectron spectroscopy. The results suggest the presence of Cu^{2+} and Cu^{3+} along with Cu^{+}. This observation is supported by cyclic voltammograms of 123 oxides recorded in a formamide medium. The valence band of 123 oxides was probed using X-ray (MgK_{α}) and ultraviolet (He–I) sources. It was observed that the Cu–O hybridized orbital in $YBa_2Cu_3O_{7-X}$ responsible for conduction decreases with time in an ultrahigh vacuum and increases with oxygen treatment temperature.

1. Introduction

The oxygen non-stoichiometry (X) is known to play an important role in the physicochemical and superconducting properties of the 123 oxides [1–3]. This has led to a number of investigations dealing with the determination of oxygen non-stoichiometry and the attendant changes in the valency of the cations, especially that of copper in these oxides. The nominal composition of the 123 oxides suggests that the valences of copper are $+2$ and $+3$. Chemical methods, like iodometry [4] and oxygen evolution methods [5–7], indicate the presence of Cu^{3+} in these oxides. However, the results obtained using spectroscopic methods like X-ray photoelectron spectroscopy (XPS) [8–13] as well as X-ray absorption spectroscopy (XAS) [14–16] are often contradictory. Thus, the lack of unambiguous experimental proof for the existence of Cu^{3+} in these oxides has either led to or supported the hypothesis that the itinerant-electron holes responsible for the high-T_C superconductivity reside primarily on the oxide ions [17, 18]. However, maintenance of oxygen non-stoichiometry near the surface of these oxides is rather difficult, especially under ultrahigh vacuum conditions in the X-ray spectrometer. Therefore, the presence of Cu^{3+} in the bulk of the cuprate superconductors has not been ruled out. The present study therefore deals with the determination of the valency of copper in the 123 oxides by X-ray photoelectron spectroscopy for freshly exposed and *in situ* high-temperature oxygen-treated samples.

For understanding the nature of conduction in these 123 oxides, studies of their electronic structures are of great importance. Therefore, the valence bands (which directly reflect the density of states near the Fermi level) of these oxides have been studied extensively [16, 19–29]. The valence band obtained using different radiation sources, contrary to expectations, shows a low density of states at the Fermi level for the 123 oxides. These results agree with the density of states obtained by band structure calculations [27, 28]. A comparison of the valence band spectra of the 123 oxide, $YBa_2Cu_3O_{7-X}$, and CuO shows that the features appearing around 3.0 to 7.0 eV arise primarily from mixed Cu3d and O2p orbitals [16, 27, 28]. However, assignments for the features in the higher binding-energy region are not clear, differing among the valence band spectra reported [16, 20]. This may be due to the fact that the spectra may not have been recorded under similar conditions, which include the time taken to record the spectra after loading the sample in the XPS chamber. Therefore, experiments carried out in the present study are not only confined to the freshly scraped surfaces but also to surfaces affected by time in an ultrahigh vacuum and by heating in an oxygen atmosphere. This allows less ambiguous assignments of the various features observed.

2. Experimental procedure

The 123 oxides were synthesized by high-temperature solid-state reaction between the constituent oxides and/or carbonates [30]. The sources for the chemicals were Ln_2O_3 (where Ln = Y, Nd, Sm, Gd or Ho), 99.9% pure (Indian Rare Earths, Kerala), $BaCO_3$, $SrCO_3$ and K_2CO_3, AR grade (Merck, India) and CuO prepared by the decomposition of $Cu(NO_3)_2 \cdot 3H_2O$, AR grade (Merck, India) at 1073 K for 10 h. The black powder of CuO was characterized by X-ray diffraction (Philips diffractometer, Model PW 1140).

Stoichiometric amounts of the constituent oxides were thoroughly mixed (using an agate mortar and pestle) and the mixture was heated in an alumina crucible at 1223 K using a silicon carbide furnace. The black powder thus obtained was made into pellets (8 or 12 mm diameter, 2–3 mm thickness) using a tungsten carbide-lined, stainless steel die and plunger (Sanvik Asia Ltd, Pune, India) under a pressure of 3–5 tonne cm^{-2}. The oxygen treatment for these pellets was given using a tubular furnace at 1173 K in flowing oxygen. The oxides thus formed were characterized by X-ray diffraction and it was found that all the 123 oxides synthesized were single-phase with orthorhombic symmetry.

0022–2461

The $NaCuO_2$ was prepared by heating stoichiometric amounts of Na_2O_2 and CuO at 543 K in flowing oxygen for 15 days [31, 32]. The model compound potassium bis(dihydrogen tellurato) cuprate (III), $K_5[Cu(H_2TeO_6)_2]$, was prepared by the method reported in the literature [33].

The X-ray photoelectron spectroscopic (XPS) studies were performed in an Escalab Mark II spectrometer (Vacuum Generators, UK) equipped with XPS and UPS facilities. The instrument also had the facility of heating the sample to a known temperature in the analyser chamber. The XP spectra were recorded using MgK_α radiation (1253.6 eV) and a pass energy of 25/50 eV. The working pressure in the analyser chamber was maintained below 5×10^{-9} torr.

Before recording the spectra, the surfaces of the samples were scraped mechanically using a stainless steel blade to avoid surface contamination. Data were either recorded directly using the output of the counter or signal-averaged, stored and then processed using an Apple II Europlus microcomputer. The peak positions were assigned by setting the adventitious carbon 1s signal to a binding energy of 285.0 eV.

In situ oxygen treatment to improve the oxygen content of $YBa_2Cu_3O_{7-X}$ was given in the preparation chamber at different temperatures ranging from 295 to 673 K at an oxygen pressure of 50 kPa for 15 min.

The ultraviolet photoelectron (UP) spectra for $YBa_2Cu_3O_{7-X}$ were also recorded using an He–I (21.2 eV) radiation source. Since the UP spectra recorded were of high intensity (20 000 counts), the changes in the features of the valence band with respect to time either in an ultrahigh vacuum (UHV) or in an oxygen atmosphere at different temperatures are small. Therefore, the difference spectra were recorded.

The cyclic voltammetric experiments were carried out after dissolving 123 oxides in formamide, using an electrochemical cell consisting of platinum wire or glassy carbon as working electrode, platinum foil as counterelectrode and silver wire as reference elctrode ($E^0_{Ag^+/Ag} = 799$ mV versus NHE). These electrodes were connected to an electrochemical analyser (Bio Analytical System model 100A, USA). The voltammograms were recorded in the potential range -1000 to $+1000$ mV, where the solvent was found to be stable. The scan rates were varied from 10 to 100 mV/s^{-1}

3. Results and discussion

The X-ray photoelectron spectra for the rare-earth substituted 123 oxides, $LnBa_2Cu_3O_{7-X}$ (Ln = Y, Nd, Sm, Gd or Ho) were recorded and the values of binding energy of various core-level peaks are given in Table I.

3.1. Copper 2p region

The Cu2p spectra of $LnBa_2Cu_3O_{7-X}$ (where Ln = Y or Nd) along with those of the reference compounds $NaCuO_2$, CuO and Cu metal are shown in Fig. 1. The Cu2p spectra of $LnBa_2Cu_3O_{7-X}$ show a main peak centred at $\simeq 933.5$ eV attributed to the presence of Cu^{2+}, which has a satellite structure ($\simeq 942$ eV) characteristic of the d^9 ground-state configuration. Moreover, the binding energy value of this peak is comparable to that of CuO. The peak at the higher binding region (> 934.5 eV) is comparable to that of $NaCuO_2$.

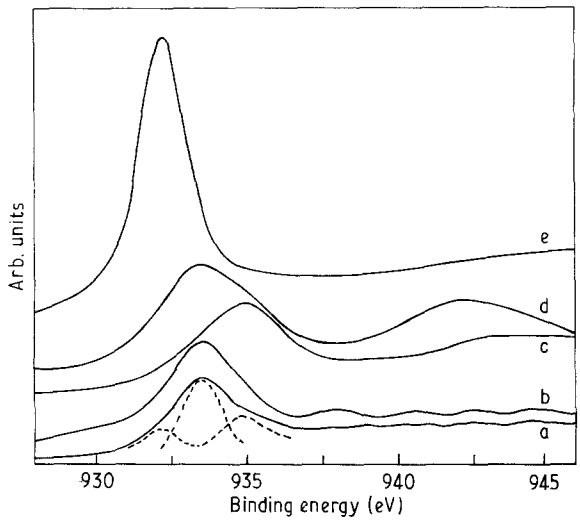

Figure 1 Copper $2p_{3/2}$ core level spectra of (a) $YBa_2Cu_3O_{7-X}$, (b) $NdBa_2Cu_3O_{7-X}$, (c) $NaCuO_2$, (d) CuO and (e) Cu metal.

TABLE I Binding energy values for core levels of all elements in $LnBa_2Cu_3O_{7-X}$

Compound	Ols	$Ba3d_{5/2}$	$Ba3d_{3/2}$	$Cu2P_{3/2}$	Ln
$YBa_2Cu_3O_{7-X}$	538.5			932.5	159.1 ($3d_{5/2}$)
	530.5	779.4	795.0	933.5	162.2 ($3d_{3/2}$)
	532.5			934.9	
$NdBa_2Cu_3O_{7-X}$	528.5	779.9	795.1	931.3	
	530.6	781.3	797.1	932.7	317.4 (4s)
	532.1			934.3	
$SmBa_2Cu_3O_{7-X}$	528.8			932.1	
	530.9	779.6	795.0	933.6	254.5 (4p)
	532.5			935.1	
$GdBa_2Cu_3O_{7-X}$	528.9			932.1	
	530.6	779.25	795.0	933.7	141.2 (4d)
	532.5			935.4	
$HoBa_2Cu_3O_{7-X}$	528.2			932.5	309.5 ($4p_{3/2}$)
	530.6	779.5	795.7	934.0	345.5 ($4p_{1/2}$)
	532.3			936.0	

Therefore, this peak is attributed to the presence of Cu^{3+}. The peak at lower binding energy (932.5 eV) is due to the presence of Cu^{+}. A similar observation is made for all the rare-earth substituted 123 oxides ($LnBa_2Cu_3O_{7-X}$). Even though there are reports contradicting the existence of Cu^{3+} in 123 oxides, the Cu2p spectra show an asymmetric peak with broadening towards the higher binding-energy region. Sacher *et al.* [13] deconvoluted the Cu2p spectra and concluded that Cu^{3+} is present in $YBa_2Cu_3O_{7-X}$. However, detection of Cu^{3+} by XPS may be difficult, mainly because the Cu^{3+} present on the surface may undergo reduction under ultrahigh vacuum conditions to Cu^{2+} or Cu^{+}. This is evident from the increase in the oxygen non-stoichiometry (X) value from 0.04 to 0.24 for $YBa_2Cu_3O_{7-X}$ samples after XPS measurement. Therefore, if the sample is kept in the XPS chamber (under UHV) for a longer time, it may not be possible to detect Cu^{3+}. Hence, in the present study, just before recording the spectra, the samples are either mechanically scraped to expose a fresh surface or oxygen-treated *in situ* at a higher temperature.

The Cu2p spectra of $YBa_2Cu_3O_{7-X}$ heated in an oxygen atmosphere at different temperatures are shown in Fig. 2. On deconvolution the intensities of the peaks corresponding to each copper ion seem to vary with temperature. The variation in the intensities of the peaks corresponding to Cu^{+}, Cu^{2+} and Cu^{3+} with oxygen treatment temperature is shown in Fig. 3. From this figure, it is evident that as the temperature of oxygen treatment increases the amount of Cu^{3+} increases and simultaneously the amount of Cu^{+} decreases. However, the trend in the intensities of these peaks seems to deviate at temperatures above 573 K. This may be due to disproportionation of the copper ions on the surface at temperatures above 573 K. These results suggest that the copper in 123 oxides is present as Cu^{2+} and Cu^{3+} along with Cu^{+}, which might have been formed due to reduction of either Cu^{2+} or Cu^{3+}.

3.2. Oxygen 1s spectra

The oxygen 1s spectra of $LnBa_2Cu_3O_{7-X}$ compounds show an asymmetric peak centred at 530.5 eV (Fig. 4).

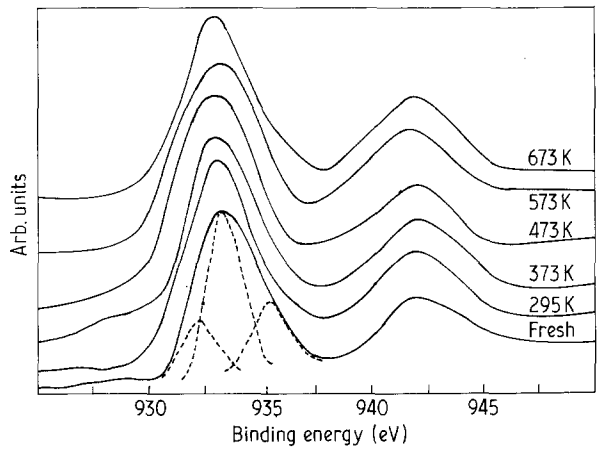

Figure 2 Copper $2p_{3/2}$ spectra of $YBa_2Cu_3O_{7-X}$ heated at different temperatures in an oxygen atmosphere.

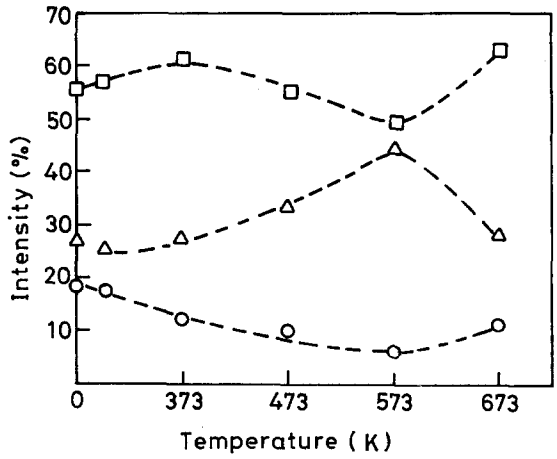

Figure 3 Variation in the intensities of the peaks of (○) Cu^{+}, (□) Cu^{2+} and (△) Cu^{3+} with oxygen treatment temperature.

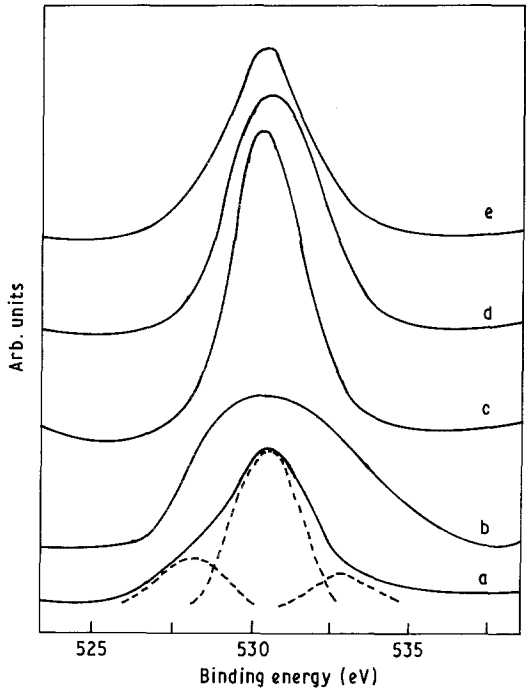

Figure 4 Oxygen 1s spectra of $LnBa_2Cu_3O_{7-X}$: Ln = (a) Y, (b) Nd, (c) Sm, (d) Gd and (e) Ho.

On deconvolution, this gives peaks at both higher ($\simeq$ 532.5 eV) and lower ($\simeq$ 528.5 eV) binding energy regions. The peaks at 528.5 and 530.5 eV seem to originate from lattice oxide ions (O^{2-}) present in two different environments, probably from Cu-O chains and planes of the 123 oxides, respectively. Weaver *et al.* [20] observed from XPS studies on single crystals of $YBa_2Cu_3O_{7-X}$ an asymmetric peak for O1s level spectra and a satellite structure (531 eV). The main peaks are attributed to Cu–O chains and planes of $YBa_2Cu_3O_{7-X}$ and the satellite structure is attributed to the final-state configuration. However, the peaks appearing at values greater than 531.0 eV are more often attributed to surface contaminants such as H_2O, OH^{-}, CO, CO_2 and also to adsorbed O_2, O^{-}, O_2^{-} (superoxide) and O_2^{2-} (peroxide), but the relationship of structural elements to specific oxygen states is yet uncertain. The carbon 1s spectrum shows a symmetrical peak centred at 285 eV, indicating that only

elemental carbon is present. Therefore, the feature observed at 532.5 eV may not be due to CO, CO_2 or carbonate. If this feature had arisen out of the emission from OH^-, H_2O and adsorbed O_2 then one would expect the intensity of these weakly bonded species to decrease with increase in the oxygen treatment temperature, but this does not seem to happen. However, species like O^-, O_2^- or O_2^{2-} may appear in this region (> 531.0 eV). However, the presence of these species in 123 oxides does not satisfy the charge neutrality principle. In this regard, Goodenough *et al.* [26] have suggested that the dimeric species O_2^{2-} could be present, but only if the oxygen content of $YBa_2Cu_3O_{7-x}$ exceeds seven oxygen atoms per formula unit. Therefore, as suggested by Weaver *et al.* [20], this peak (532.5 eV) would have arisen due to the final-state configuration ($O2p^5L$).

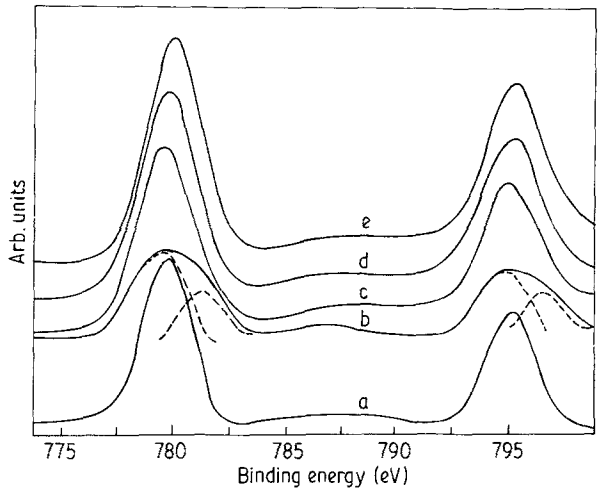

Figure 5 Barium 3d spectra of $LnBa_2Cu_3O_{7-x}$: Ln = (a) Y, (b) Nd, (c) Sm, (d) Gd and (e) Ho.

3.3. Barium 3d region

The barium 3d spectra ($3d_{3/2}$ and $3d_{5/2}$) of the 123 oxides $LnBa_2Cu_3O_{7-x}$ are shown in Fig. 5. Except for $NdBa_2Cu_3O_{7-x}$, all other rare-earth substituted 123 oxides show symmetric peaks suggesting that only one type of barium species (Ba^{2+}) is present. The Ba3d spectrum of $NdBa_2Cu_3O_{7-x}$ shows an asymmetric peak suggesting that barium ion is present in two different chemical environments. Most likely, barium may be present as Ba^{+2+d} (d-oxygen deficiency) along with Ba^{2+}. Mingrong *et al.* [21] have also observed two peaks in the Ba3d region and have suggested that the presence of oxygen-deficient barium ions is possible in these ceramic oxides. These results are consistent with the exceptional behaviour of $NdBa_2Cu_3O_{7-x}$ among the rare-earth substituted 123 oxides.

The core-level spectra corresponding to Y3d, Nd4s, Sm4p, Gd4d and Ho4p show symmetric peaks indicating the presence of only one kind of rare-earth ion in these 123 oxides, which is in conformity with the crystal structure.

3.4. The valence-band region

The valence-band spectra obtained using X-ray (MgK_α) radiation for the 123 oxides are shown in Fig. 6. For comparison the density of states for $YBa_2Cu_3O_{7-x}$ obtained by band structure calculations by Park *et al.* [34] is shown in Fig. 7. It is evident from these figures that the features around 3.0 to 7.0 eV are mainly due to hybridized Cu3d and O2p orbitals. The effective overlap of the copper and oxygen orbitals is very crucial for superconductivity in these copper-based oxides. This is evident from the photoemission studies on the copper based oxides by Steiner *et al.* [28]. Their studies show that the valence-band spectra of $YBa_2Cu_3O_{7-x}$ show a single peak between 3.0 and 7.0 eV, whereas the valence-band spectra of Cu_2O and CuO show distinguishable peaks at 3.0 and 7.0 eV, suggesting that the Cu3d and O2p orbitals are not effectively overlapping as in $YBa_2Cu_3O_{7-x}$. However, the valence-band spectra of semiconducting $YBa_2Cu_3O_6$ and superconducting

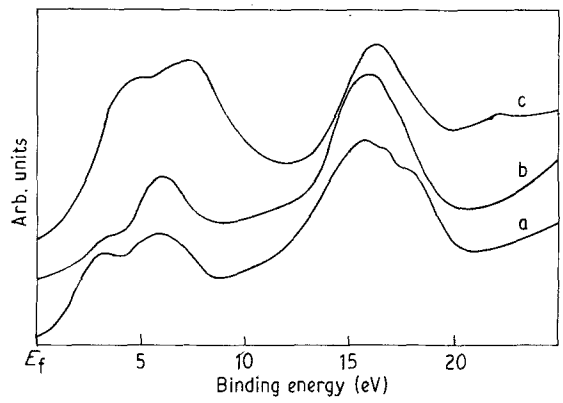

Figure 6 Valence-band spectra of $LnBa_2Cu_3O_{7-x}$ obtained with MgK_α radiation source: Ln = (a) Y, (b) Sm and (c) Gd.

$YBa_2Cu_3O_7$ show a similar structure at the Fermi level, even though one would expect them to be different [35].

As mentioned earlier, the oxygen non-stoichiometry in $YBa_2Cu_3O_{7-x}$ is found to increase after XPS measurements. This shows that the sample loses oxygen under ultrahigh vacuum conditions. Therefore, to understand the effect of a vacuum on the valence band of $YBa_2Cu_3O_{7-x}$, the UV photoelectron spectra (He–I, $E = 21.2$ eV) were recorded at different time intervals (5, 10, 15, 30 and 60 min) in an ultrahigh vacuum (10^{-9} torr) and at room temperature. It was noticed that the changes in the feature in the valence band were small with time in a vacuum; therefore the difference spectra (i.e. difference between the spectrum recorded at time t' and the spectrum recorded at $t' = 0$) are shown in Fig. 8. It is seen that the intensity of the feature at 3.0 to 7.0 eV (as indicated by an arrow) corresponding to the Cu–O hybridized orbital decreases with time in UHV. Moreover, the peaks become separated, indicating a decrease in the effective overlap between Cu3d and O2p orbitals.

Further, to confirm the above observation, the UV spectra were recorded for $YBa_2Cu_3O_{7-x}$ heated *in situ* in an oxygen atmosphere (0.5 atm) at different temperatures ranging from 295 to 673 K. The difference spectra for these oxygen-treated samples are

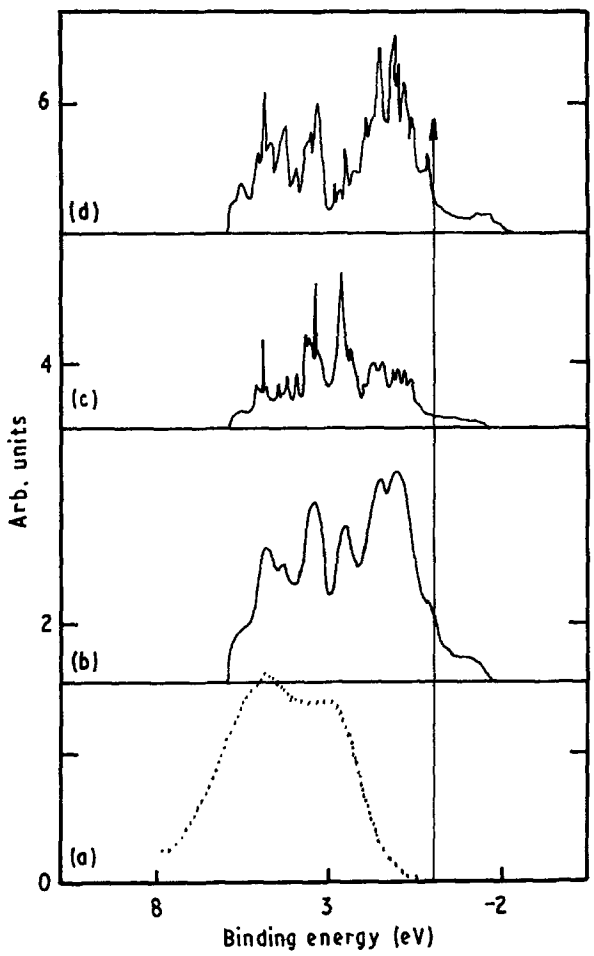

Figure 7 Comparison of results for local density of states obtained by band structure calculation and a valence band spectrum obtained using He–II radiation for $YBa_2Cu_3O_{7-x}$. (a) Valence-band spectrum obtained with He–II radiation, (b) total density of states, (c) Cu3d-derived density of states, (d) O2p-derived density of states [34].

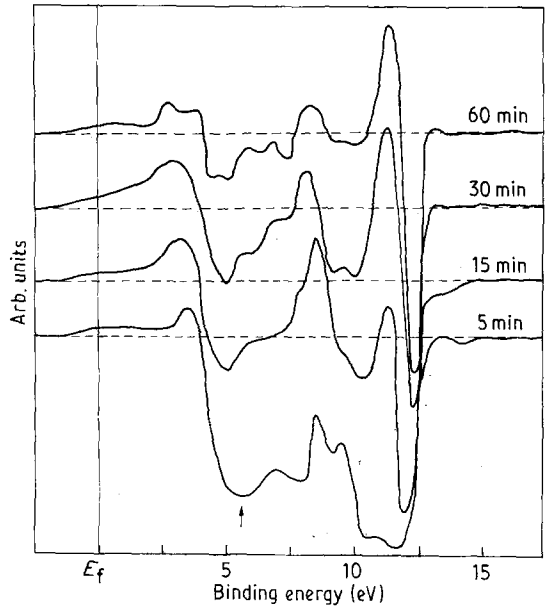

Figure 8 Difference spectra (UPS) of $YBa_2Cu_3O_{7-x}$: difference between the spectrum recorded at time t' in ultrahigh vacuum and the spectrum recorded at time $t' = 0$.

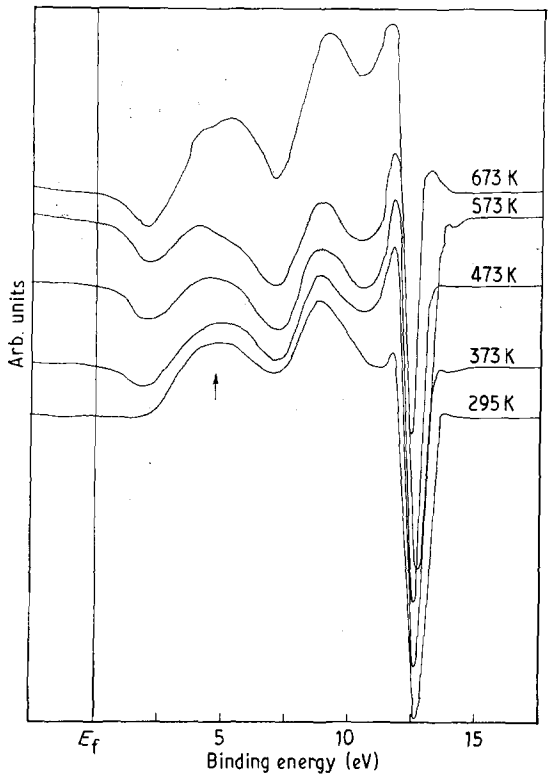

Figure 9 Difference spectra (UPS) of $YBa_2Cu_3O_{7-x}$: difference between the spectra recorded at different temperatures in oxygen atmosphere and the fresh spectrum.

shown in Fig. 9. It is seen that the intensity of the feature at 3.0 to 7.0 eV (as indicated by an arrow) increases as the oxygen treatment temperature increases. This suggests that the effective overlap between Cu3d and O2p orbitals increases with an increase in temperature. It is known that an increase in the oxygen treatment temperature increases the oxygen content in 123 oxides and hence increases the conductivity. Therefore, the Cu–O hybridized orbital plays an important role in the superconductivity of the copper-based oxide superconductors.

3.5. Cyclic voltammetric measurements

A typical voltammogram of the 123 oxide is shown in Fig. 10a. The voltammogram shows two cathodic reduction peaks (c_1 and c_2) followed by two anodic oxidation peaks (a_1 and a_2). Similar voltammograms were observed for all the 123 oxides; however, the peak positions were found to shift marginally (Table II).

In the cathodic sweep, the first reduction peak appears approximately at -100 mV (versus Ag^+/Ag). This peak is attributed to the reduction of Cu^{3+} to Cu^{2+}. This is because the equilibrium potentials of Cu^{2+} and Cu^+ reductions are more negative than the potential observed for Cu^{3+} reduction, and also because other metal ions present in the 123 oxides are not reducible under these conditions. The redox potential of the Cu^{3+}/Cu^{2+} couple has been examined by a number of groups for copper (III) complexes with peptides and dithiocarbamates as ligands [36–39]. The redox potentials reported are in the range $+500$ to $+1000$ mV (versus NHE) and the value reported by Latimer [40] also is in the same range. However, it

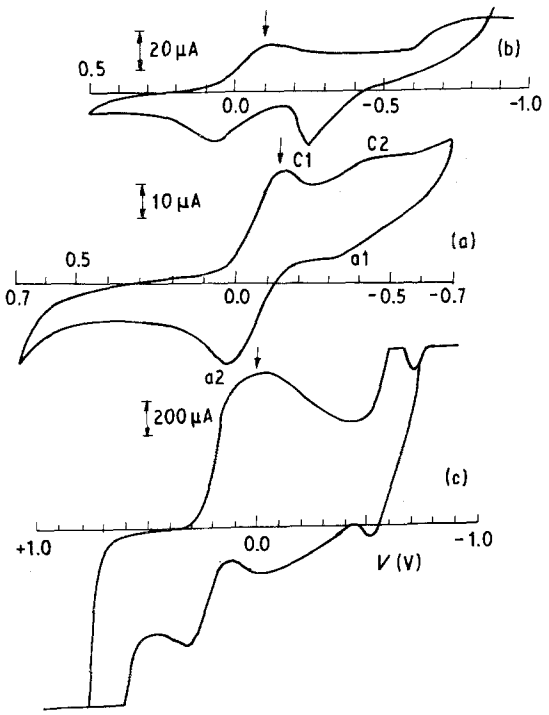

Figure 10 Cyclic voltammograms (versus Ag/Ag^+) of (a) $YBa_2Cu_3O_{7-X}$, (b) $NaCuO_2$ and (c) $K_5[Cu(H_2TeO_6)_2]$.

TABLE II Redox potentials of $LnBa_2Cu_3O_{7-X}$ in formamide using different working electrodes and silver wire (+ 799 mV versus NHE) as reference electrode at a scan rate of 10 mV s^{-1}

Ln	Redox potential (mV) E_p^{c1}	E_p^{a2}	E_p^{c2}	E_p^{a1}
Platinum wire electrode				
Y	− 170	+ 60	− 650	− 60
Nd	− 90	+ 210	− 660	+ 110
Gd	− 100	+ 30	− 720	− 50
Sm	− 70	− 20	− 680	+ 100
Ho	− 80	+ 110	− 520	+ 40
Glassy carbon electrode				
Y	− 120	+ 20	− 450	− 320
Nd	− 120	+ 110	− 500	− 360
Gd	− 100	− 20	− 490	− 350
Sm	− 120	+ 40	− 460	− 360
Ho	− 130	+ 30	− 450	− 340

should be remarked that the large variation in the reported values of the redox potential for Cu^{3+}/Cu^{2+} has to be associated with the nature of the medium, the ligand, the supporting electrolyte and the working electrode.

Even though the redox potential values of the Cu^{3+}/Cu^{2+} couple observed for these 123 oxides are in the range reported in the literature, in order to establish this further the cyclic voltammograms of compounds containing copper exclusively in the 3 + state, namely $NaCuO_2$ and $K_5[Cu(H_2TeO_6)_2]$, were recorded. The voltammograms of these compounds along with that of $YBa_2Cu_3O_{7-X}$ are shown in Fig. 10b and c. It is seen that the first reduction peak in all three voltammograms appears in the same range of potential. These results clearly show that Cu^{3+} is also present in the 123 oxides. Moreover, recently Chen *et al.* [41] have recorded cyclic voltammograms for $YBa_2Cu_3O_{7-X}$ with different X values using 1.0 M $LiClO_4$–propylene carbonate as well as saturated $Ba(OH)_2$ as electrolytes, and then determined Cu^{3+} in $YBa_2Cu_3O_{7-X}$. The Cu^{3+}/Cu^{2+} redox potential (− 800 mV versus SCE) obtained by these authors is in close agreement with the value obtained in the present study.

Normally, cyclic voltammograms are recorded by sweeping the potential first in the cathodic direction followed by the anodic direction. Even when the above order of sweeping the potential was reversed, the anodic oxidation peak (a_1) appeared in the case of $YBa_2Cu_3O_{7-X}$, whereas this peak was absent in the voltammograms of CuO and $NaCuO_2$. This shows that the 123 oxide contains Cu^+. However, the peak intensity is found to be small and is found to increase in subsequent scans. These results suggest that apart from Cu^{2+} and Cu^{3+}, Cu^+ is also present in these 123 oxides. The Cu^+ could have been formed due to reduction of Cu^{3+} or Cu^{2+}.

4. Conclusions

The X-ray photoelectron spectra of Cu2p emission in 123 oxides show a main peak at 933.5 eV along with peaks at 934.5 and 932.5 eV. This result suggests that the copper in 123 oxides is present as Cu^{2+} along with Cu^{3+} and Cu^+. It has been suggested in this connection that Cu^{3+} would be present at the Cu1 site (copper in the Cu–O chains) and Cu^{2+} would occupy the Cu2 site (copper in the Cu–O planes). Therefore, the ground-state configuration for Cu–O chain is $Cu3d^82p^6$ or $Cu^{3+}O^{2-}$ and the planar Cu–O is $(Cu3d^92O2p^6)L$ or $(Cu^{2+}O^{2-})^+$, where L represents a hole in the Cu–O hybridized orbital. Thus the O1s peak appearing at 528.5 eV is attributed to the $Cu3d^8O2p^6$ configuration (oxygen present in the Cu–O chains) and the peak at 530.5 eV is attributed to $(Cu3d^9O2p^6)L$ (oxygen present in the Cu–O planes). However, it has also been suggested that Cu–O is present in the $Cu3d^9O2p^5L$ or $Cu^{2+}O^-$ configuration [42]. Such a configuration does not satisfy the charge neutrality principle for the 123 oxide. The cyclic voltammograms obtained for these 123 oxides also indicate the presence of Cu^{2+} and Cu^{3+} along with Cu^+. The UP spectra of $YBa_2Cu_3O_{7-X}$ suggest that the intensity of the Cu3d–O2p hybridized orbital responsible for conduction decreases with time in a vacuum and increases with oxygen treatment temperature.

Acknowledgement

One of the authors (N.S.R.) thanks CSIR, New Delhi for the financial assistance and RSIC, IIT, Madras for recording photoelectron spectra.

References

1. R. J. CAVA, B. BATTLOG, C. H. CHEN, E. A. RIETMANN, S. M. ZAHURAK and D. WERDER, *Nature* **329** (1987) 423.
2. P. K. GALLAGHER, H. M. O'BRYAN, S. A. SUNSHINE and D. W. MURPHY, *Mater. Res. Bull.* **22** (1987) 995.

3. "Chemical and Structural Aspects of High Temperature Superconductors", edited by C.N.R. Rao (World Scientific, Singapore, 1988).
4. D. C. HARRIS and T. A. HEWSTON, *J. Solid State Chem.* **69** (1987) 182.
5. G. KAWAMURA and M. HIRATANI, *J. Electrochem. Soc.* (1987) 3211.
6. D. C. PARASHER, J. RAI, P. K. GUPTA, R. C. SHARMA and K. LAL, *Jpn. J. Appl. Phys.* **27** (1988) L2304.
7. S. X. DOU, H. K. LIU, A. J. BOURDILLON, N. SARRIDES, J. P. ZHOU and S. S. SORREL, *Solid State Commun.* **68** (1988) 47.
8. P. STEINER, V. KINSINGER, I. SANDER, B. SIEGUART, S. HUFFNER, C. POLITIS, R. HOPPE and H. P. MULLER, *Z. Phys. B* **67** (1987) 497.
9. N. T. LIANG, K. H. LI, Y. C. CHOU, M. F. TAI and T. T. CHEN, *Solid State Commun.* **64** (1987) 761.
10. N. MORI, Y. TAKANO and H. OZAKI, *Jpn. J. Appl. Phys.* Suppl. 26-3 (1987) BJ21.
11. D. D. SHARMA and C. N. R. RAO, *Solid State Commun.* **65** (1988) 47.
12. R. SCHLOGL, H. EICKENBUSCH, W. PAULUS and R. SCHOLLHORN, *Mater. Res. Bull.* **24** (1989) 181.
13. E. SACHER, J. E. KLEMBERG-SAPIEHA, A. CAMBRON, A. OKANIEWSKI and A. YELON, *J. Elect. Spect. Relat. Phenom.* **48** (1989) C7.
14. A. BIANCONI, A. CONGIU CASTELLANO, M.DE SANTIS and R. RUDOLF, *Solid State Commun.* **63** (1987) 1009.
15. F. BANDELET, G. COLLIN, E. DARTUGE, A. FONTAINE, J. P. KAPPLER, G. KRILL, J. P. ITIE, J. JEGOUDEZ, M. MAURER, Ph. MONOD, A. REVCOLEVSCHI, H. TOLENTINO, G. TOURILLON and M. VERDAGUER, *Z. Phys.* **B69** (1989) 149.
16. E. Z. KURMAUV and L. D. FINKELSTEIN, *Int. J. Mod. Phys.* **B3** (1989) 973.
17. V. J. EMERY, *Phys. Rev. Lett.* **58** (1987) 2794.
18. J. B. GOODENOUGH, *Mater. Res. Bull.* **23** (1983) 401.
19. M. G. RAMSEY and F. P. NETZER, *Mater. Sci Engng* **B2** (1989) 269.
20. J. H. WEAVER, H. M. MEYER III, T. J. WAGENER, D. M. HILL and Y. GAO, *Phys. Rev.* **B38** (1988) 4668.
21. J. MINGRONG, H. ZHENGHUI, W. JIANXAN, Z. HAN, P. GUPGIANG, C. ZHUYAO, Q. YITAI, Z. YONG, H. LIPING, X. JIANSEN and Z. QIRUI, *Solid State Commun.* **63** (1987) 511.
22. W. R. FLAVELL and R. G. EDGEL, *Supercond. Sci. Technol.* **1** (1988) 118.
23. T. HASHESEMI, F. GOLESTANI-FARD, Z. T. ALDHHAN and C. A. HOGARTH, *Spectrochim. Acta* **43B** (1988) 951.
24. S. MYHRA, J. C. RIVIERE, A. M. STEWART and P. C. HEALY, *Z. Phys. B. Condensed Matter* **72** (1988) 413.
25. C. N. R. RAO, P. GANGULY, J. GOPALAKRISHNAN and D. D. SARMA, *Mater. Res. Bull.* **22** (1987) 1159.
26. J. B. GOODENOUGH, A. MANTHIRAM, Y. DAI and A. CAMPION, *Supercond. Sci. Technol.* **1** (1988) 187.
27. W. E. PICKETT, *Rev. Mod. Phys.* **61** (1989) 433.
28. P. STEINER, S. HUFFNER, A. JUNGMANN, V. KINSINGER and I. SANDER, *Z. Phys. B. Condensed Matter* **74** (1989) 173.
29. J. C. FUGGLE, P. J. W. WEIJS, R. SCHOORL, G. A. SAWATZKY, J. FINK and N. NUCKER, P. J. DURBAM and W. M. TEMMERMAN, *Phys. Rev.* **B37** (1988) 123.
30. R. J. CAVA, B. BATTLOG, R. B. VAN DOVER, D. W. MURPHY, S. SUNSHINE, T. SIEGRIST, J. P. REMEIKA, S. ZAHRAUK and G. P. ESPINOSA, *Phys. Rev. Lett.* **56** (1987) 1676.
31. W. KLEMM, G. WEHREMEYER and H. BADE, *Z. Electrochem.* **63** (1959) 56.
32. K. HESTERMAN and R. HOPPE, *Z. Anorg. Allgem. Chem.* **367** (1978) 261.
33. S. CHANDRA and K. L. YADAVA, *Talenta* **15** (1968) 349.
34. K. T. PARK, K. TERAKURA, T. OGUCHI, A. YANAE and M. IKEDA, *J. Phys. Soc. Jpn* **57** (1988) 3445.
35. R. G. EGDELL and W. R. FLAVELL, *Z. Phys. B. Condensed Matter* **74** (1989) 279.
36. F. P. BOSSU, K. L. CHELLAPPA and D. W. MARGERUM, *J. Amer. Chem. Soc.* **99** (1977) 2195.
37. M. P. YOUNGBLOOD and D. W. MARGERUM, *Inorg. Chem.* **19** (1980) 3068.
38. P. R. SHARP and A. J. BARD, *ibid.* **22** (1983) 3462.
39. P. S. ZACHARIAS and A. RAMACHANDRAN, *Polyhedron* **4** (1985) 1013.
40. N. M. LATIMER, "The Oxidation States of the Elements and their Potentials in Aqueous Solutions" (Prentice Hall, New York, 1964) p. 188.
41. L. Q. CHEN, Y. Z. HUANG, L. Z. XIN, X. J. HUANG and T. E. HUL, *Bull. Electrochem.* **5** (1989) 483.
42. P. SALVADOR, J. L. G. FIERRO, J. AMADOR, C. CASCALES and I. RASINES, *J. Solid State Chem.* **81** (1989) 240.

Received 30 July 1991
and accepted 11 March 1992